J. Adhesion Sci. Technol., Vol. 9, No. 7, pp. 935–951 (1995)

Cation diffusion at the polymer coating/metal interface

JAMES POMMERSHEIM,[1] TINH NGUYEN,[2,*] ZHUOHONG ZHANG[1] and CHANGJIAN LIN[†]

[1]*Chemical Engineering Department, Bucknell University, Lewisburg, PA, USA*
[2]*National Institute of Standards and Technology, Gaithersburg, MD 20899, USA*

Received in final form 3 February 1995

Abstract—Theoretical and experimental studies were carried out on the transport of cations in the channel between a polymer coating and a metal substrate from a defect in the absence of an applied electrical potential. The model consists of two stages: an initial period during which ions diffuse in the coating/metal interfacial 'channel' and adsorb on the coating surface, and a propagation period during which ions also diffuse into the coating. The mathematical models were solved to predict the cation concentration and flux under the coating and the relative rate of diffusion between the initial and propagation periods. Model parameter values were derived from the results of an experiment conducted in a specially designed diffusion cell. The experiment measured the depletion of Na^+ ions in a cylindrical, central reservoir, which was placed within the perimeter of a defect through the coating of an epoxy-coated steel panel. Model predictions of concentration versus time agreed well with the experimental results, which showed that most of Na^+ ions were removed by lateral diffusion from the reservoir during the initial period. Further, the transport during the initial period was much faster than that during the propagation period. The results also indicated that during the propagation period, the rate-limiting step was the lateral diffusion along the coating/metal interface rather than diffusion through the coating.

Keywords: Cation ions; coating; defect; diffusion; model; polymer/metal interface.

NOTATION

a	radius of the inner cylinder
C_A	concentration of sodium ions in the channel between the coating the metal substrate
C_a	sodium ion concentration within the inner cylinder
C_{a0}	initial concentration of sodium ions
C'_{a0}	value of C_a at $t = \Theta_i$
C_{Aw}	concentration of sodium ions in the outer cylinder

*To whom correspondence should be addressed.
†Present address: Chemistry Department, Xiamen University, Fujian, People's Republic of China.

D_c effective diffusivity of sodium ions through the coating from the interface

D_e effective diffusivity of sodium ions under the coating

f dimensionless function defined by equation (21)

H height of cylinders

h coating thickness

m dimensionless modulus,

$$m = \sqrt{\frac{D_c}{D_e}\frac{R^2}{h\delta}}$$

N_r radial flux of sodium ions

R radius of the outer cylinder

r radial coordinate

r_i radius of the moving interface

Δr width of thin shell in the channel located at radius r

t time

V volume of solution in the inner cylinder

V_w volume of water in the outer cylinder

y dimensionless radius, r_i/a

w_A molar flow rate of sodium ions

Greek letters

α reciprocal of the system time constant for model I,

$$\alpha = \frac{\delta D_e C_{a0}}{a^2} = \frac{\pi D_e \delta}{V\gamma}$$

α' reciprocal of the system time constant for model II,

$$\alpha' = \frac{2\pi a \delta D_c \eta}{Vh}$$

γ dimensionless adsorption parameter in model I,

$$\gamma = \frac{\rho_s \pi a^2}{V C_{a0}}$$

δ effective height of the channel

ρ_s surface molar density of the adsorbed layer

η ion penetration parameter,

$$\eta = \frac{2af}{R^2 - a^2}\sqrt{\frac{hD_e\delta}{D_c}}$$

Θ dimensionless concentration, $(C_A - C_{Aw})/(C_a(t) - C_{Aw})$
Θ_i time for end of first period and start of second
τ_I time constant for model I
τ_{II} time constant for model II
ξ dimensionless radius, r/R

1. INTRODUCTION

Corrosion of metals beneath organic coatings is a problem of major importance to coating technologists. In order for corrosion to occur, there must be sources of oxygen, water, and an electrolyte to transfer charge. When the corrosion occurs beneath the coating, these chemicals can be transferred by diffusion or an applied or induced potential to the corrosion site. Any of a number of processes may control the overall corrosion rate, but diffusion of chemical species is always a likely candidate to limit transport because it is inherently a slow process. Typical diffusion rates through coatings are orders of magnitude less than their unhindered values.

Migration of cations can occur by diffusion between anodic and cathodic corrosion sites at the interface between the coating and the metal. These sites may initially be close to one another, but with time they can separate and become localized. Cathodic blisters can form and eventual coating failure may result. The transport of cations such as sodium provides a mechanism to neutralize the hydroxide ions [1–4]:

$$O_2 + 2H_2O + 4e^- + 4Na^+ = 4\left(Na^+OH^-\right).$$

In the presence of an applied or induced potential, diffusion is facilitated. It is possible to produce concentrations within cathodic blisters which are many times greater than their values in the external solution. This has been observed experimentally and predicted theoretically [5–7]. The model of Pommersheim *et al.* [7] involves two periods: an initiation period and a propagation period. During the initiation period, ions diffuse through the channel between the coating and the substrate. An advancing front where cations are instantaneously removed by sorption is predicted to move between the anode and the cathode. During the propagation period, cations break through into the cathodic blister, where they accumulate. During both periods, the applied potential facilitates the diffusion process. A critical value of the potential was predicted below which blisters would not grow and above they would.

In this paper the transport of cations (sodium ions) in the channel between an organic coating and a metal substrate is studied in the absence of an applied electrical potential. Both diffusion along the coating/metal interface and diffusion outward through the coating (in the axial direction) are considered, as well as adsorption of sodium ions on the underside of the coating.

2. EXPERIMENTAL

2.1. Specimen preparation

Figure 1 presents a schematic diagram of the specimen configuration for the measurement of the diffusion of cations at the organic coating/steel interface. It consists of an organic-coated substrate, an inner glass cylinder containing a solution of sodium chloride, and a large, outer cylinder holding distilled water. The substrate was an SAE 1010, cold-rolled steel, and the organic coating was a commercial, two-component, room-temperature cure, pigmented epoxy formulation. The resin was a diglycidyl ether of bisphenol A and the curing agent was a polyamide adduct. The total pigment content (by mass) in the coating was 42.5%. The substrate has a matte finish and surface roughness ranging from 0.9 to 1.3 μm. The substrate, having dimensions of 152 × 102 × 0.8 mm, was cleaned by repeatedly and alternately rinsing with acetone and methanol (reagent grades), followed by hot, dry air. The coating was applied on the substrate immediately after drying, using the draw-down technique. Excess coating was placed on one end of the substrate panel and then pulled down along the length of the panel using a glass rod. Masking tape strips, 5 mm wide, placed along the length of the panel edges were used to control the coating thickness. The coating was allowed to cure at room conditions (24 °C and 45% relative humidity) for 2 weeks. The thickness of the coating was approximately 150 μm, as determined by an eddy current gage. The equilibrium water uptake in the cured coating was approximately 2.5% (based on dry coating material), as determined gravimetrically.

After curing, a disk of 13 mm in diameter of the coating from the center of the panels was bored to the steel substrate and removed from the coated panel. A glass tube (inner cylinder), having an outside diameter of 12.5 mm, an inner diameter of 12 mm, and a height of 50 mm, was placed where the coating disk was removed (Fig. 1). Epoxy adhesive was used to seal the space between the glass tube and the coating. A 0.05-mm-thick gasket made of poly(tetrafluoroethylene), having an outside diameter of 13 mm and an inside diameter of 10 mm, was situated at the bottom of the glass tube. This procedure ensured that the epoxy adhesive did not come into

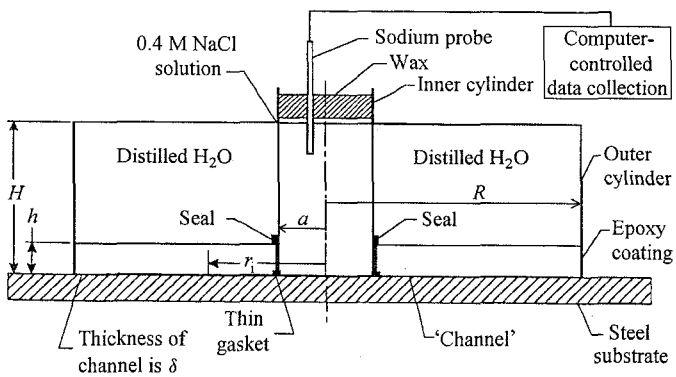

Figure 1. Specimen configuration for measuring the diffusion of cations beneath an organic coating on a substrate.

contact with the steel substrate, which could have blocked the lateral diffusion route of cations. Using a room-temperature-cure silicone adhesive, an open-ended, PMMA cylinder (outer) was attached to the coated substrate, symmetrically around the inner cylinder. Both the height and the inner diameter of the outer cylinder had the same dimension, 50 mm.

2.2. Measurement of the cation concentration

The diffusion of cations in the 'channel' between the coating and the metal substrate was measured by following the decrease of Na^+ ion concentration in the inner cylinder. The concentration of Na^+ ions in the inner cylinder was measured using a commercial, 1 mm tip, Na^+-miniselective electrode. The electrode was connected to a high-impedance ($>10^{14}$ Ω) ion analyzer. The ion analyzer was programmed to record Na^+ ion concentrations at desired intervals. The ion-selective electrodes respond to activity rather than concentration, where activity is related to the concentration by the activity coefficient. However, because the measurement system was calibrated in terms of concentration, we reported our results in terms of concentration. The Na^+-selective electrode was calibrated prior to the actual measurements and its reliability was ensured by checking at the conclusion of the experiment. A preliminary experiment indicated that in order to maintain the same liquid volume in the inner cylinder throughout the measurement, the coated substrate within the outer cylinder must be soaked in water for 24 h. For that reason, doubly distilled water was placed in the outer cylinder 24 h prior to filling the inner cylinder with the cation-containing solution, a 0.4 mol/l solution of NaCl in doubly distilled water. Thus, it was assumed that there was a water layer at the coating/substrate interface within the area covered by the outer cylinder prior to filling the inner cylinder with the cation solution [8, 9].

The top of the inner cylinder was sealed with molten wax and cellophane film was used to cover the top of the outer cylinder (Fig. 1). This procedure was used to minimize the evaporation of water from both cylinders. The duration of the experiment was 174 h. There was little change in the liquid levels in both the inner and the outer cylinders during this period. There was some corrosion on the bare steel area inside the inner cylinder. Further, at the end of the experiment, the coating was easily detached from the substrate, indicating that the adhesion was completely lost after the experiment. However, the metal underneath the coating was still bright and showed no evidence of corrosion. The data collected together with the specimen characteristics are presented in the Appendix.

3. CONCEPTUAL MODEL FOR CATION DIFFUSION ALONG THE COATING/METAL INTERFACE

The sodium ions diffuse from the inner chamber (Fig. 1) into 'channel' which lies between the coating and the metal substrate. In the absence of an applied electrical potential, this transport mode is believed to be the main process responsible for the delamination of organic-coated metals containing a defect exposed to an electrolyte [2–4, 10]. The transport process is presumed to occur in two stages or periods. During

the first period, ions diffuse through the channel to a point (r_i) where they are rapidly removed by adsorption onto the bottom surface of the coating. This process defines a moving interface (located at r_i), which advances under the coating. The initiation period ends at time Θ_i when the interface reaches the far end of the coating ($r = R$). During the second or last period, which begins at time Θ_i, lateral diffusion along the interface still occurs, but this time the sink for the ions is diffusion of ions into the coating from the channel. Thus, in this period diffusion occurs in two directions: along the coating/metal interface (radial direction) and normal to the coating (axial direction). This transport is assumed to occur by a first-order process, so that where the concentration of ions in the channel is higher, more diffusion into the film will occur. During both periods, ions are being removed from the solution in the inner cylinder, but during the first period ions are removed more rapidly since the diffusion distances are smaller. Thus, the second stage should occur over time periods longer than the first.

Since higher concentrations of sodium are present near the entrance of the channel (at $r = a$), more transport into the coating will occur there. The amount of adsorption and diffusion into the coating will depend on the thicknesses of the channel and coating, the cell dimensions, and the diffusivity of sodium ions through the channel and coating. These factors will also determine whether transport is controlled by diffusion along the coating/metal interface or through the coating.

4. MATHEMATICAL MODEL FOR CATION DIFFUSION ALONG THE COATING/METAL INTERFACE

4.1. Model I (initial stage)

During the initial stage, cations A (considered to be sodium ions here) are diffusing under the influence of a concentration gradient. The concentration of sodium ions is $C_a(t)$ at $r = a$ and zero at $r = r_i$, where they are removed by rapid adsorption. This establishes a linear concentration gradient.

The molar flow of A, w_A, is given by

$$w_A = -2\pi r \delta D_e \frac{dC_A}{dr} = -2\pi \delta D_e \frac{\int_{C_a}^{0} dC_A}{\int_{a}^{r_i} \frac{dr}{r}} = \frac{2\pi \delta D_e C_a}{\ln \frac{r_i}{a}}, \tag{1}$$

where C_A is the concentration of sodium at any radius r in the channel, a is the radius of the inner cylinder, δ is the height of the channel, and D_e is the effective diffusivity of sodium ions in the channel.

At steady state, the diffusive flow must be equal to the rate at which sodium ions are adsorbed or bound to the surface:

$$w_A = -\rho_s \frac{dr_i}{dt} 2\pi r_i, \tag{2}$$

where ρ_s is the surface molar density (mol/cm^2) of sodium ions in the adsorbed layer.

Equating equations (1) and (2) gives

$$-\rho_s \frac{dr_i}{dt} = \frac{\delta D_e C_a(t)}{r_i \ln \frac{r_i}{a}}. \tag{3}$$

The concentration of sodium ions $C_a(t)$ within the inner chamber can be found from an ion balance at $r = a$:

$$-V\frac{dC_a}{dt} = w_A|_{r=a} = -D_e \frac{\partial C_A}{\partial r}\bigg|_{r=a} 2\pi a\delta, \tag{4}$$

where V is the volume of solution in the inner cylinder.

The sodium ion concentration can be found as a function of r_i by accounting for the total amount of adsorbed sodium ion:

$$C = \frac{C_a}{C_{a0}} = 1 - \frac{\rho_s \pi a^2}{V C_{a0}}\left[\left(\frac{r_i}{a}\right)^2 - 1\right], \tag{5}$$

where C_{a0} is the initial sodium ion concentration in the inner cylinder and C is the dimensionless concentration.

Substituting equation (5) into equation (3) leads to

$$\int_1^y \frac{y \ln y \, dy}{(1+y) - \gamma y^2} = \frac{\delta D_e C_{a0}}{\rho_s a^2} t = \alpha t, \tag{6}$$

where y is the dimensionless distance r_i/a, and

$$\gamma = \frac{\rho_s \pi a^2}{V C_{a0}}. \tag{7}$$

α, the reciprocal of the time constant for the initial period, is given by

$$\alpha = \frac{\delta D_e C_{a0}}{\rho_s a^2} = \frac{\pi D_e \delta}{V\gamma}. \tag{8}$$

Equations (5) and (6) can be used together to predict the concentration of sodium ions within the inner cylinder as a function of time. The initial stage ends when $t = \Theta_i$ at $y = R/a$. For fixed values of the parameters α and γ, equation (6) can be used to predict Θ_i. As indicated by equation (7), γ is a dimensionless parameter which is a measure of the amount of adsorption which can occur.

4.2. *Model II (final stage)*

The second or final stage begins when the first stage ends (at $t = \Theta_i$). During this stage, diffusion occurs both along the coating/metal interface and into the coating. This model was developed by first making a sodium ion balance on a thin shell in the channel located at radius r and having width Δr, which leads to

$$2\pi r \delta N_r\big|_r - 2\pi \delta N_r\big|_{r+\Delta r} - \frac{2\pi r \Delta r D_c (C_A - C_{Aw})}{h} = 0, \tag{9}$$

where δ is the height of the channel, N_r is the radial flux of sodium ions, D_c is the diffusivity of sodium ions through the coating, h is the coating thickness, and C_{Aw} is the concentration of sodium ions in the outer cylinder.

In the limit $\Delta r \longrightarrow 0$, we obtain

$$-\frac{d(rN_r)}{dr} = \frac{rD_c}{h\delta}(C_A - C_{Aw}), \tag{10}$$

so that

$$\frac{1}{r}\frac{d}{dr}\left(r\frac{dC_A}{dr}\right) = \frac{D_c}{h\delta D_e}(C_A - C_{Aw}). \tag{11}$$

In the above formulation, several assumption are implicit. The flux of sodium ions into the coating is taken equal to $D_c(C_A - C_{Aw})/h$. This formulation presumes that a linear concentration gradient of cations across the coating is rapidly established and maintained, a situation which is made more likely because the coating is thin. In addition, the diffusivities D_c and D_e are taken to be constant. This is a reasonable assumption considering the uniformity of the coating and the fact that the free stream or bulk diffusivity is relatively independent of concentration for sodium chloride solutions [11]. Also, since the amount of water in the outer cylinder is more than ten times that of the solution in the inner cylinder (see the Appendix), C_{Aw} will remain low compared with C_A.

Equation (11) is subject to the boundary conditions

$$C_A = C_a(t) \quad \text{at } r = a$$

and

$$\frac{\partial C_A}{\partial r} = 0 \quad \text{at } r = R.$$

The last condition arises because there should be few or no Na^+ ions migrating beyond the end of the channel (at $r = R$) (underneath the wall of the outside cylinder). The relatively small area here ($2\pi\delta R$) ensures that only a small number of ions will be transported there as compared with those that pass into the much larger area beneath the coating.

Equation (10) and the boundary conditions can be made dimensionless by the substitutions

$$\Theta = \frac{C_A - C_{Aw}}{C_a(t) - C_{Aw}} \tag{12}$$

and

$$\xi = \frac{r}{R}, \tag{13}$$

leading to

$$\frac{1}{\xi}\frac{\mathrm{d}}{\mathrm{d}\xi}\left(\xi\frac{\mathrm{d}\Theta}{\mathrm{d}\xi}\right) = \frac{D_c}{h\delta D_e}R^2\Theta = m^2\Theta \tag{14}$$

with the dimensionless conditions

$$\Theta = 1 \quad \text{at } \xi = \frac{a}{R}$$

and

$$\frac{\mathrm{d}\Theta}{\mathrm{d}\xi} = 0 \quad \text{at } \xi = 1.$$

Alternatively, equation (14) can be written as

$$\xi^2\Theta'' + \xi\Theta' - \xi^2 m^2\Theta = 0, \tag{15}$$

where

$$m^2 = \frac{D_c}{D_e}\frac{R^2}{h\delta}. \tag{16}$$

The dimensionless parameter m is a measure of the relative importance of diffusion along the coating/metal interface to diffusion through the coating. If m is large, diffusion along the interface will control transport, while if m is small, diffusion through the coating will control. Because the geometric ratio $R^2/h\delta$ will, in general, be quite large for a typical coating system, if the diffusion coefficients are of comparable magnitude, diffusion along the interface is more likely to control transport.

The solution of equation (15) is given in terms of modified Bessel functions:

$$\Theta = c_1 I_0(m\xi) + c_2 K_0(m\xi). \tag{17}$$

Applying the boundary conditions, the constants c_1 and c_2 can be found, so that

$$\Theta = \frac{K_1(m)I_0(m\xi) + I_1(m)K_0(m\xi)}{K_1(m)I_0\left(m\frac{a}{R}\right) + I_1(m)K_0\left(m\frac{a}{R}\right)}. \tag{18}$$

Equation (18) governs the dimensionless concentration profile within the channel during the final stage.

As shown by equation (4), a sodium ion balance on the inner cylinder equates the depletion of sodium ions to the amount that diffuses out through the channel entrance (at $r = a$). The gradient $\mathrm{d}C_A/\mathrm{d}r$ at $r = a$ is found by differentiating equation (18). Performing this operation and simplifying gives

$$-V\frac{\mathrm{d}C_a}{\mathrm{d}t} = 2\pi\frac{a\delta\eta}{h}D_c C_a, \tag{19}$$

where the parameter η is given by

$$\eta = \frac{2af}{R^2 - a^2}\sqrt{\frac{hD_e\delta}{D_c}} \tag{20}$$

with

$$f = \frac{I_1(m)K_1(m\,a/R) - K_1(m)I_1(m\,a/R)}{K_1(m)I_0(m\,a/R) + I_1(m)K_0(m\,a/R)}. \tag{21}$$

Equation (19) is integrated to give the sodium ion concentration as a function of time:

$$\frac{C_a}{C'_{a0}} = \exp\left[-\frac{2\pi a\delta D_c\eta}{Vh}(t - \Theta_i)\right] = e^{-\alpha'(t-\Theta_i)}, \tag{22}$$

where C'_{a0} is the concentration of sodium ions at the start of the final stage ($t = \Theta_i$). α', the reciprocal of the system time constant for model II, is given by:

$$\alpha' = \frac{2\pi a\delta D_c\eta}{Vh}. \tag{23}$$

Equation (22) predicts that the concentration will fall exponentially for times greater than Θ_i. Together with equations (5) and (6), which are valid for times less than Θ_i, it governs the way that the concentration of sodium ions within the inner cylinder varies with time. Model constants can be determined by fitting experimental data to these equations.

5. RESULTS AND DISCUSSION

The data given in the Appendix for the sodium ion at different times within the inner cylinder can be used to evaluate the best values of the model constants α and γ (for model I) and α' (for model II). For the range of experimental data reported, γ must lie between 0 and 0.0765.

The initiation time Θ_i depends on both α and γ since from equation (6)

$$\int_1^{\frac{R}{a}} \frac{y \ln y\, dy}{(1 + y) - \gamma y^2} = \alpha\Theta_i. \tag{24}$$

α, α', and γ were found by minimizing the overall sum of squares of the deviations between the observed and predicted concentrations for both models. A numerical simulation was used to evaluate the integrals in equations (6) and (24). The computer programs for these operations are given in [12].

The best values of the model constants for this method were found to be $\alpha = 9.5 \times 10^{-3}$ h^{-1}, $\alpha' = 5.0 \times 10^{-3}$ h^{-1}, and $\gamma = 0.065$. Using these values, Θ_i was

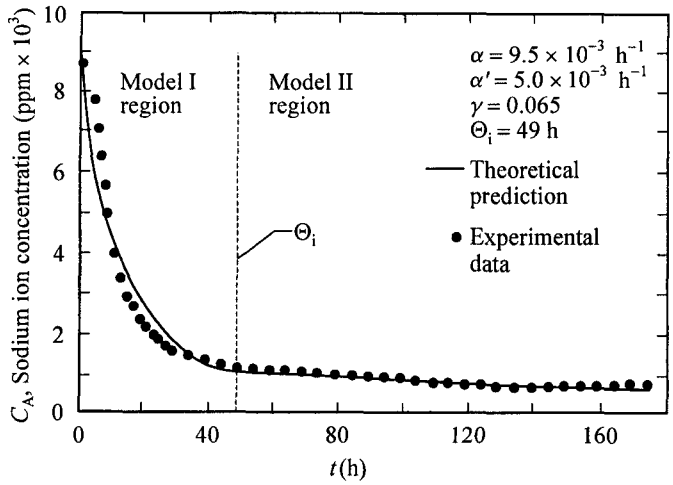

Figure 2. Comparison of the predicted with the experimental values of sodium ion concentration at the defect as a function of time (C_a vs. t).

evaluated as 49 h by using equation (24). Figure 2 is a plot which compares the original data with those predicted by the models. A good fit is obtained for model II, while for model I, for times less than Θ_i, the fit is not as good. One reason for the disparity may be due to an electro-osmotic flow of water, which accompanied the transport of Na^+ ions [13]. This additional water flow would likely decrease the Na^+ ion concentration in the channel and thus increase the rate of Na^+ ion transport from the outside to the channel.

A second possible reason for the lack of a good fit between the theoretical and experimental data at early times is unsteady state effects associated with the initial penetration of sodium ions into the channel. Both models assume that diffusion occurs at a quasi-steady state, so that concentrations within the channel have enough time to continually readjust to the changing concentrations within the inner cylinder. However, there may be a small initial period during which a quasi-steady state is not yet established. The epoxy coating will take a short time to become acclimated to the first sodium ions which enter the channel. During this period, rapid adsorption may occur. Diffusion into the coating can also be slowed down by the accumulation of sodium ions in the distilled water in the outer cylinder; thus, the assumption that $C_{Aw} = 0$ will not be valid at longer times. Although no measurement on the concentration of Na^+ ions in the outer cylinder was done to verify this assumption, diffusion coefficients of cations through organic coatings have been reported to be in the 10^{-9}–10^{-13} cm^2/s range [3, 14, 15]. Even if no adsorption occurred, the highest value of C_{Aw} could only reach 688 ppm under the experimental conditions employed. With adsorption removing the bulk of sodium, the highest value of C_{Aw} would fall to 107 ppm.

Another factor that may affect the rate of transport of ions along the interface from the defects is the galvanic potential produced by the corrosion reactions at the defects. This factor was not investigated in this study. However, by using a novel

approach, Stratmann *et al.* [4] demonstrated that a substantial potential gradient can exist between the active metal surface at the defect exposed to an electrolyte and the intact coating/metal interface. This potential gradient decreases with distance from the defect. They further reported that this unintentional, induced potential influences the transport of cations along the coating/metal interface. In a study where an electrical potential was applied between the defects and the cathodic blisters, we found that above a critical value, potential is the main factor driving cations from the defects to the cathodic blisters [5, 6]. Indeed, the the concentration of Na^+ ions in the blister after 800 h under an −875 mV potential (vs. Ag/AgCl reference electrode) between a scribe mark and a simulated cathodic blister was more than five times that of the exposed 0.5 mol/l solution. It is noted, however, that in this experiment only the defect was exposed to the electrolyte solution while the simulated blister initially contained only de-ionized, distilled water.

The ratio of the constants α/α' is a measure of the constants τ_{II}/τ_I, where τ_{II} is the time constant for model II and τ_I is the time constant for model I. For the experimental data obtained (see the Appendix), this ratio is 1.9, indicating that the initial diffusion and adsorption of ions in the channel occur on a time scale about twice as fast as their subsequent diffusion into the coating. The value $\gamma[(R/a)^2 - 1]$ is the amount of sodium ions that can adsorb in the channel relative to the amount that is potentially available for adsorption. For the experiment conducted this is 0.85, and from the Appendix the matching concentration occurs at about 42 h. This indicates that the coating adsorbs all but 15% of the sodium ions available within that time. The remainder is then available to diffuse into the coating. Note that the models predict that this will occur in 49 h.

From the best values of α and γ, the diffusion coefficient–channel depth product $D_e\delta$ is 1.71×10^{-7} cm^3/s. The ease with which the epoxy coating could be detached from the steel substrate at the conclusion of the experiment suggests that δ may be large. For an average channel width of $\delta = 0.1$ mm, this would give an effective lateral diffusivity of $D_e = 1.71 \times 10^{-5}$ cm^{-2}/s, which is close to the free stream value for sodium chloride, 1.5×10^{-5} cm^{-2}/s [11], and three times higher than that of Na^+ ions through an ion-exchange membrane [16, 17].

Figure 3 presents a plot of the parameter η versus the modulus m. a/R is shown as a parameter. η is a quantitative measure of the penetration of ions. It is the ratio of the molar flow (mol/s) of ions beneath the coating to the maximum flow, which would occur if the whole underside of the coating could be exposed to solution having the external concentration C_{a0}. It is a dimensionless measure of how effective the coating is in removing cations. η values lie between 0 and 1. Small values of m yield large η values (~ 1), while at large values of m, η becomes small. With the maximum flow, there are no concentration gradients beneath the coating and the modulus m is small. As shown by the figure, η is then close to unity. In general, when $m < 0.5$, diffusion through the coating will control transport, while if $m > 2$, diffusion along the coating/metal interface will control. In the transition region $0.5 < m < 2$, neither mechanism will dominate. Figure 3 delineates the three regions.

Higher values of a/R result in higher values of η for same modulus. η is larger because, for the same R, the diffusion distances under the coating are shorter, so

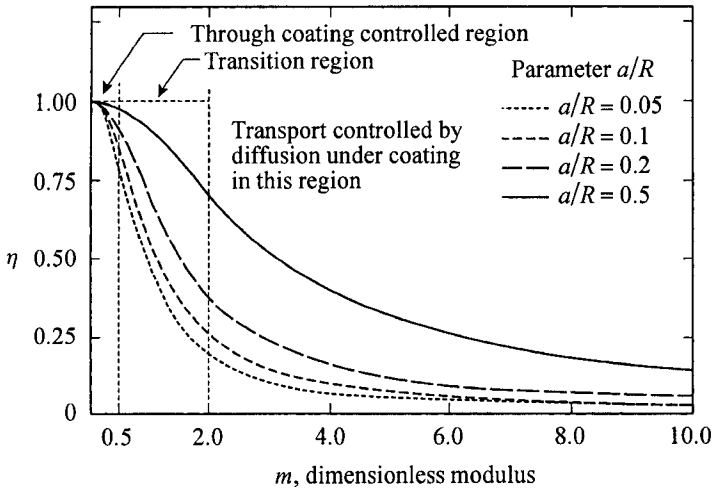

Figure 3. Plots of η versus the dimensionless modulus m. (See the Notation for definitions of η and m.)

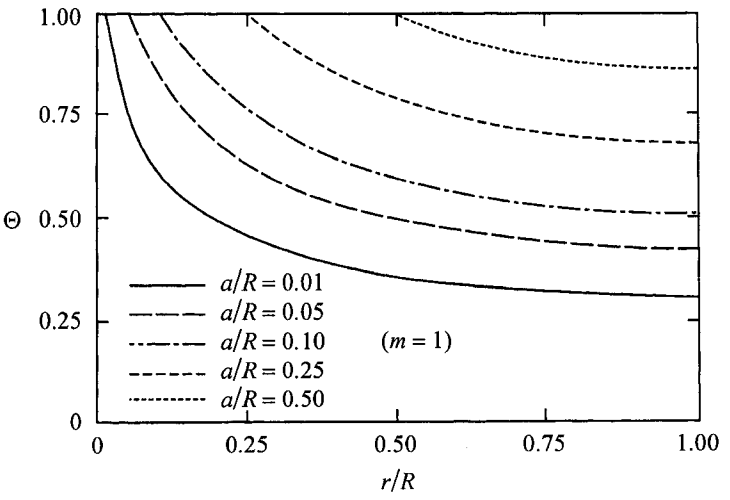

Figure 4. Plots of dimensionless concentration Θ versus the aspect ratio r/R for $m = 1$.

that concentrations remain closer to the value in the inner solution. This is shown in Fig. 4 ($m = 1$) for where the slope of the dimensionless concentration profiles is less at higher values of a/R. In Fig. 5, higher values of m result in steeper predicted profiles. The second curve from the right shows the approximate profile predicted by the model for the experimental conditions employed.

Since $D_e\delta$ and a/R are known, equations (16), (20), and (21) can be solved iteratively for the values of D_c, m, and η, yielding $D_c = 7.4 \times 10^{-8}$ cm^2/s, $m = 12.1$, and $\eta = 0.055$. Although the D_c value is several orders of magnitude higher than the values of organic coatings that were measured by the ion flux techniques [3, 14, 15], it is in the same range (2.5×10^{-8} cm^2/s) as that obtained using the transient current

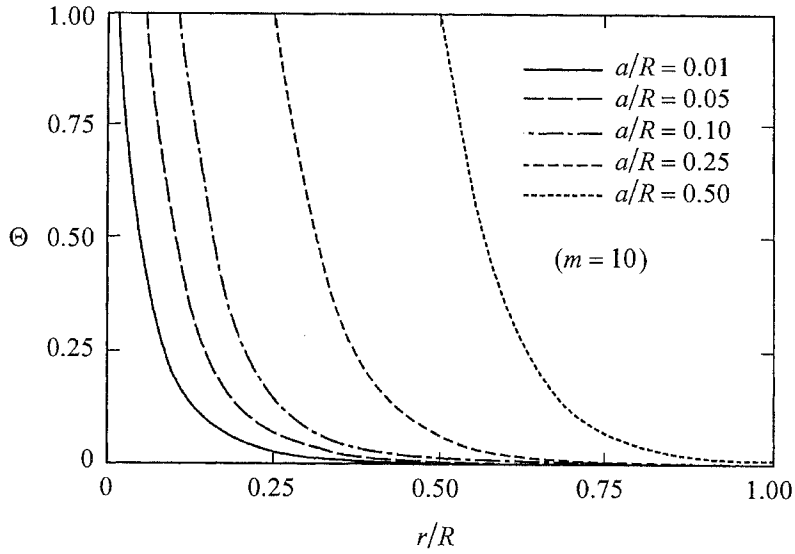

Figure 5. Plots of dimensionless concentration Θ versus the aspect ratio r/R for $m = 10$.

data [15]. Ruggeri and Beck [15] attributed the three-order magnitude discrepancy between the values determined by the two techniques for a polyurethane film to the presence of additional mobile ions, which provides a medium for the flow of current.

Another possible explanation for the higher outward diffusion coefficient of Na^+ obtained in this study is due to the alkaline environment produced by the corrosion process at the coating/steel interface. The alkaline environment would increase the water uptake and internal stresses in the coatings, both of which would facilitate the transport of ions through the coating film. The alkalinity is a product of the corrosion activity under the coating near the defects. This comes about because the bare metal at a large defect or a scribe mark of a polymer-coated steel undergoes anodic reactions (corrosion) and the area underneath the coating surrounding the defect undergoes cathodic reactions [1–4, 18–20]. In the absence of an applied electrical potential, sodium ions are believed to migrate along the coating/steel interface from the defect to the cathodic sites [2–4, 10] to neutralize the hydroxyl ions, which are produced by the cathodic reactions, forming NaOH. In the presence of a potential applied across the coated panel, Leidheiser [19] maintained that cation transport through the coating film is the limiting step. Thus, the liquid at the coating/steel interface near the defects is highly alkaline. Indeed, pH values close to 14 have been measured at these sites [20]. The alkalinity of the liquid at the coating/metal interface can cause the disbondment of a coating from a metal surface. This phenomenon is commonly known as cathodic delamination. As stated in Section 2, we observed corrosion at the bare metal in the inner cylinder. It is likely that the cathodic delamination occurred underneath the coating surrounding the inner cylinder. This was evidenced by the complete detachment of the film from the substrate and the bright appearance of the

substrate after the film was removed at the conclusion of the experiment. This may provide a partial explanation for the relatively high δ value derived from the model.

The alkaline environment at the coating/steel interface may induce stresses in the epoxy coatings by two possible mechanisms. The first mechanism is the development of an osmotic pressure gradient between the outside water environment and the coating/steel interface. As indicated earlier, the area underneath the coating near the defect underwent cathodic reactions and this area is rich in highly hygroscopic NaOH corrosion products. As a result, the water activity of the external solution is higher than that at the coating/steel interface, creating an osmotic pressure difference between the outside and the inside. Consequently, water flows into the coating, creating a pressure that counterbalances the water in-flow. Inside the coating, the pressure generated by the swelling process produces an elastic stretching of the polymer. Swelling pressures in the range of several hundred kg/cm^2 have been reported for polyamide-cured epoxy films when they absorb water [17]. Since the osmotic pressure gradient is a function of the water activity in the outside environment, the use of distilled water in the outer cylinder in the present study should facilitate maximal water uptake by the coating and the film should stretch to its greatest extent.

Another mechanism whereby the alkaline environment at the coating/steel interface may induce stresses in the coatings is through an increase of the fixed charges in the coating, which are produced during the curing process [17]. The sign and concentrations of these fixed charges alter substantially when the environment in contact with the coatings changes from neutral and acidic to basic. Since osmotic pressure is directly related to the concentration of fixed charge in the coatings [17], the alkaline environment at the coating/steel interface is expected to increase the swelling pressure in the coating. More hydrophilic polymers tend to swell more because the stronger polar or ionic-water interactions in these materials will cause a greater free energy decrease. The existence of internal stresses in swollen polymers and their effect on transport have been documented [21, 22]. In the presence of swelling pressure, the diffusion of penetrant has been found to be a linear function of time (instead of the square root of time as with classical diffusion). This type of diffusion is frequently accompanied by fracture of the material. In some polymers, the internal stresses generated during diffusion were so large that the films cracked [21].

The relatively high value of m and the corresponding low value of η both indicate that diffusion along the coating/metal interface is the rate-limiting step for the transport of sodium ion during the final stage. Note, however, that the ratio of the diffusivity in the channel to that in the coating (D_e/D_c) is quite high (from 23 to 230, depending on the value of δ). Diffusion is effectively two-dimensional when most of the ions pass completely underneath the coating before they start to diffuse through it. In general, this would occur with a low value of m. For the conditions employed in the present experiment, the high value of the geometric factor $R^2/h\delta$ makes m relatively high, so that diffusion will not be two-dimensional. This can also be seen in Fig. 5, where under the experimental conditions employed the concentration is predicted to fall towards zero only at a short distance from the inner cylinder. The steep concentration gradients indicate that the principal diffusional resistance occurs in the channel under the coating.

6. CONCLUSIONS

Mathematical models were developed and solved for the two-stage transport of ions by diffusion beneath and through organic coatings. During the first stage, transport occurred by radial diffusion in the channel between the coating and the metal substrate with rapid adsorption on the coating underside surface. During the second stage, diffusion also occurred outward through the coating. Model parameters were obtained from an experiment conducted in a specially designed diffusion cell in which the depletion of sodium ions in a central reservoir was measured. Model predictions of concentration versus time agreed well with the experimental results. Most of the sodium ions were removed during the first stage, as indicated by the relatively high value of the adsorption parameter γ. The first stage occurred more rapidly than the second, as indicated by the ratio of time constants for the two periods. High values of the dimensionless modulus m indicated that during the second stage, cation transport was controlled by diffusion in the channel between the coating and the metal substrate rather than by diffusion through the coating, even though the diffusivity of ions under the coating was much higher than that for ions through the coating.

REFERENCES

1. W. Schwenk, in: *Corrosion Control by Organic Coatings*, H. Leidheiser, Jr (Ed.), p. 103. National Association of Corrosion Engineers, Houston, TX (1981).
2. T. Nguyen, J. B. Hubbard and G. B. McFadden, *J. Coatings Technol.* **63** (794), 43 (1991).
3. W. Funke, *Ind. Eng. Chem. Prod. Res. Dev.* **24**, 343 (1985).
4. M. Stratmann, A. Leng and W. Furbeth, in: *Proc. XXth Int. Conf. on Coatings Sci. Technol.*, Athens, Greece, p. 519 (1994).
5. J. M. Pommersheim, T. Nguyen, Z. Zhang, C. Lin and J. B. Hubbard, Technical Note 1293, National Institute of Standards and Technology (May 1992).
6. T. Nguyen and J. M. Pommersheim, *Proc. Mater. Res. Soc. Symp.* **304**, 14 (1993).
7. J. M. Pommersheim, T. Nguyen, Z. Zhang and J. B. Hubbard, *Prog. Org. Coatings* **25**, 23 (1994).
8. T. Nguyen, E. Byrd and C. Lin, *J. Adhesion Sci. Technol.* **5**, 697 (1991).
9. T. Nguyen, D. Bentz and E. Byrd, *J. Coatings Technol.* **66** (834), 39 (1994).
10. H. Leidheiser, Jr, W. Wang and L. Igetoft, *Prog. Org. Coatings* **11**, 19 (1983).
11. R. Robinson and R. Stokes, *Electrolytic Solutions*, 2nd edn. Academic Press, New York (1959).
12. J. M. Pommersheim, T. Nguyen, Z. Zhang and C. Lin, Internal Report NISTIR 5102, National Institute of Standards and Technology (April 1993).
13. G. W. Castellan, *Physical Chemistry*, 2nd edn, p. 439. Addison-Wesley, Menlo Park, CA (1971).
14. A. L. Glass and J. Smith, *J. Paint Technol.* **38**, 203 (1966).
15. R. T. Ruggeri and T. R. Beck, in: *Corrosion Control by Organic Coatings*, H. Leidheiser, Jr (Ed.), p. 62. National Association of Corrosion Engineers, Houston, TX (1981).
16. M. J. Pikal and G. E. Boyd, *J. Phys. Chem.* **77**, 2918 (1973).
17. H. Corti and R. Fernandez-Prini, *Prog. Org. Coatings* **10**, 5 (1982).
18. R. A. Dickie, in: *Polymeric Materials for Corrosion Control*, R. A. Dickie and F. L. Floyd (Eds), Am. Chem. Soc. Symp. Series No. 322, p. 136. American Chemical Society, Washington, DC (1986).
19. H. Leidheiser, Jr, *Corrosion* **39**, 189 (1983).
20. J. J. Ritter and J. Kruger, in: *Corrosion Control by Organic Coatings*, H. Leidheiser, Jr (Ed.), p. 28. National Association of Corrosion Engineers, Houston, TX (1981).
21. T. Alfrey, E. E. Gurnee and W. G. Lloyd, *J. Polym. Sci.* **C12**, 249 (1966).
22. T. K. Kwei and H. M. Zupko, *J. Polym. Sci.* **A2**, 867 (1969).

APPENDIX: EXPERIMENTAL DATA

Specimen characteristics

Radius of inner cylinder	$a = 0.6$ cm
Radius of outer cylinder	$R = 2.25$ cm
Thickness of coating	$h = 150\ \mu\text{m} = 1.5 \times 10^{-2}$ cm
Height of solutions in cylinders	$H = 3$ cm
Volume of NaCl solution in inner cylinder	$V = 3.39$ ml
Volume of distilled water in outer cylinder	$V_w = 44.23$ ml

Concentration C_a (ppm) of sodium ions within the inner cylinder as a function of time

$C_{a0} = 9000$ ppm

Time (h)	C_a (ppm)	Time (h)	C_a (ppm)	Time (h)	C_a (ppm)
0	9000	29	1650	109	863
1	8760	34	1520	114	830
5	7800	39	1400	119	814
6	7050	44	1310	124	804
7	6390	49	1210	129	774
8	5690	54	1170	134	744
9	5000	59	1160	139	730
11	4020	64	1150	144	718
13	3420	69	1120	149	721
15	2990	74	1090	154	724
17	2710	79	1020	159	718
19	2410	84	1000	164	724
21	2220	89	988	169	721
23	2000	94	954	174	721
25	1870	99	929		
27	1730	104	880		